Low Latency Single-Cycle EOG Classification Using Cascaded ANN & CNN

Article · June 2025

DOI: 10.1109/ICCIT64611.2024.11022078

5 authors, including:

Abdullah Bin Shams
University of Toronto
58 PUBLICATIONS **499** CITATIONS
SEE PROFILE

Md Rifatuddin Romel
Military Institute of Science and Technology
1 PUBLICATION **0** CITATIONS
SEE PROFILE

Mohammad Liton Hossain
Institute of Science and Technology
20 PUBLICATIONS **26** CITATIONS
SEE PROFILE

2024 27th International Conference on Computer and Information Technology (ICCIT)
20-22 December 2024, Cox's Bazar, Bangladesh

Low Latency Single-Cycle EOG Classification Using Cascaded ANN & CNN

Wakim Sajjad Sakib[1], Abdullah Bin Shams[2*], Md. Rifatuddin Romel[3], Raisa Tasrin Ridi[4], Mohammad Liton Hossain[5]

[1]*Dept. of Electronics and Communication Engineering, Institute Of Science and Technology, Dhaka 1209, Bangladesh*
[2]*Dept. of Electrical & Computer Engineering, University of Toronto, Toronto, Ontario M5S 3G4, Canada*
[3]*Dept. of Aeronautical Engineering, Military Institute of Science and Technology, Dhaka 1216, Bangladesh*
[4]*Dept. of Computer Science and Engineering, American International University - Bangladesh, Dhaka 1229, Bangladesh*
[5]*Department of Electrical and Electronic Engineering, University of Dhaka, Dhaka 1000, Bangladesh*
*Corresponding author: abdullahbinshams@gmail.com

***Abstract*—Electrooculography (EOG) is a noninvasive method to record the motion of the eye from the electrical potential difference between the cornea and retina. This technique, paired with AI, is extensively utilized predominantly in assistive technologies. The complexity of AI-driven EOG analysis scales with the number and type of expected eye movements. This challenge intensifies when the detection of eye movements relies solely on a single EOG cycle. An essential metric for real-time applications is the latency of an AI algorithm, which refers to the delay in making predictions. The latency should be smaller than the average human visual reaction time for any AI-driven system to promptly respond. The majority of EOG classification studies tend to overlook latency. In this experimental study, we overcome this multi-facet problem by proposing cascaded Artificial Neural Network (ANN) and Convolutional Neural Network (CNN) architectures that have latency smaller than average human reaction time. Also, we developed a generalized & robust signal processing method to correctly identify single EOG cycle and deliver high prediction performances with either ANN or CNN. To demonstrate, we successfully classified nine distinct eye movements based only on single cycle EOG signal, with the performance metrics reaching close to 100% for both ANN & CNN, and latency well below the reaction time.**

***Index Terms*—Single cycle EOG classification, Latency, Human-computer interaction, Smart Wearable devices, ANN, CNN.**

I. Introduction

Human-Computer Interaction (HCI) is a key research area where pattern recognition plays a crucial role. Recognizing patterns in bioelectrical signals drives progress in wearable smart technologies. Electrooculography (EOG) measures electrical potential between the cornea and retina, generated by eye movements, through electrodes placed around the eyes. EOG signals are resilient against neuromuscular impairments like spinal cord injuries and Locked-in Syndrome, making EOG-based HCI devices highly beneficial for patients with severe motor disabilities. This makes EOG essential in advancing assistive technologies.

Recently, AI-powered wearable devices have gained attention for their ability to adapt to user behavior, enhancing personalized healthcare technologies. AI provides advanced signal processing techniques that can extract relevant features from complex, overlapping signals, making it more effective for EOG signal processing than traditional hardware implementations. Various AI-integrated wearable EOG applications have been developed, including wheelchair control [1], alcohol detection via smart glasses [2], robotic arm maneuvering for Tetraplegia patients [3], computer mouse control [4], and sleep stage identification in both healthy and hospitalized individuals [5].

Classification of EOG signals is a critical task in HCI, as it is essential for precise control of wearable devices. Recent advancements in EOG research have introduced several innovative approaches for eye movement classification. Support Vector Machines (SVM) have been used to identify four gaze directions (right, left, up, and down), achieving an accuracy of 99% [1]. Another study employed wavelet transform combined with supervised learning algorithms, such as K-Nearest Neighbors (KNN), SVM, and Decision Trees (DT) algorithms, to classify five eye movements (left, right, down, up, blink) from two-channel EOG signals. This approach achieved classification accuracy of 69.4%, 76.9%, and 60.5%, respectively [6]. Another study was conducted to predict eight directional eye movements (up, down, left, right, up-left, up-right, down-left, down-right) from four-channel EOG signals but confronted challenges with blink detection due to the variations in the signal amplitude [7]. 1D CNN has been used to classify a four-channel EOG signal. This approach eliminates the need for manual feature extraction and achieves an accuracy of 98.70% for horizontal directions and 80.94% for vertical directions [8]. An EOG-controlled prosthetic hand was designed that achieved error rates of 0% (right and left), 36% (top), 4% (bottom), and 16% (front) across ten subjects after five trials per eye movement [9]. Kabir et al. used SVM and MLP to classify EOG data for controlling a computer mouse cursor via eye movements. Their model achieved an average classification accuracy of up to 93% across all directions [10]. Another similar study employed RNN-GRU and Bidirectional GRU to classify four directional movements (up, down, left, right) [11]. Their

979-8-3315-1909-4/24/$31.00 © 2024 IEEE

combined model achieved an accuracy of 99.77% and 99.74% for vertical and horizontal channels, respectively. Reda et. al used ResNet-50 to classify six eye movement directions (Right, left, up, down, center, and double blinking) [12]. Their approach demonstrated a high level of accuracy, achieving an average of 95.8%. None of the aforementioned studies classified EOG signals from single-cycle electrooculograms, nor did they address the latency of the prediction algorithms, which is crucial for creating a seamless wearable device. Additionally, they reported accuracy without clarifying whether they referred to training or validation accuracy.

In this experimental study, we investigate the use of ANN and CNN to classify nine distinct eye movements based on single-cycle, two-channel EOG signals, achieving high validation accuracies. The identified ocular movements include: blink, left, right, up, down, up-left, up-right, down-left, and down-right. This comprehensive set is critical for sophisticated smart technology applications. ANN is chosen for its ability to model complex non-linear relationships, while CNN is selected for its translation invariance. The latency of these algorithms is influenced by factors such as model design, complexity, and the choice of activation functions. Our objective is to harness the strengths of these algorithms and design neural network architectures capable of predicting faster than the average human visual reaction time of 250 ms [13]. Moreover, we demonstrate that our signal preprocessing technique is compatible with both ANN & CNN to classify eye movements from a single-cycle EOG with an overall latency shorter than the reaction time. This advancement could enable automatic interpretation of reactive movements, a critical feature in applications such as brain-computer interfaces, robotic-assisted surgeries, and driver assistance systems, where immediate and accurate control is essential [14]–[16].

II. Methods and Materials

This section outlines the key procedures of our experimental study, which is illustrated in Fig. 1.

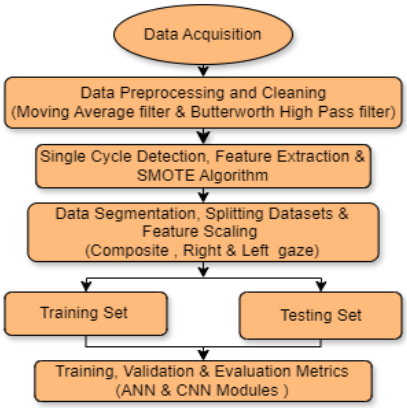

Fig. 1. Work flow of the study.

A. Data acquisition

At the KUET biomedical laboratory, EOG signals representing nine distinct eye movements (blink, up, down, left, right, down-left, down-right, up-left, and up-right) were recorded from 20 participants with equal representation of genders. The recordings were made using the Biopac MP3X system. The experimental setup involved using high-quality equipment, including electrolyte gel, disposable electrodes, electrode lead cables, connection cables, a power transformer, a BIOPAC MP3X Acquisition Unit, a desktop computer, power cables, LED, connecting wires, an Arduino board, 9V battery, and a buzzer. Data was collected with a sampling frequency of 125 Hz using six disposable electrodes, four for horizontal and vertical movements and the remaining two for reference, as shown in Fig. 2.

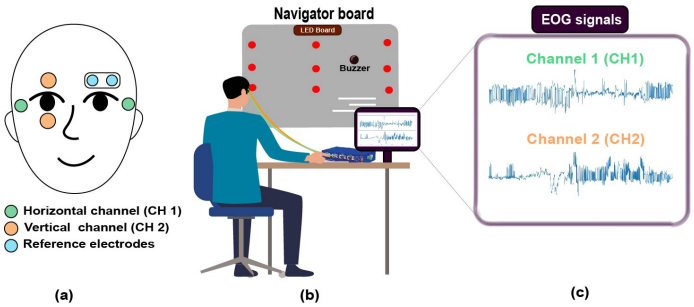

Fig. 2. (a) Electrode placement to record two-channel EOG signal; (b) Experimental setup of our study; (c) Acquired signals

B. Data processing

Bioelectrical signals often exhibit noise, artifacts, and low-frequency drifts (trends), which can obscure true EOG patterns. To resolve these issues, a two-step filter operation was done. At first, the moving average low-pass filter was used to reduce the noise and artifacts by removing unwanted high-frequencies. Subsequently, a Butterworth high-pass filter was employed to remove the low-frequency drift.

C. Single-cycle detection & Feature extraction

To identify individual cycles, a function was developed to identify peaks by monitoring when the amplitude surpasses a specific threshold in both upward and downward directions, indicating the start and end of that particular cycle. The midpoint of these two points is then considered as a peak. To optimize the peak detection we used a minimum peak distance parameter that allows the function to capture more accurate peaks as illustrated in Fig. 3. We then collected data points from each side of the peaks to identify individual cycles.

From individual cycles, we extracted the following key features: 1)Maximum value, 2) Minimum value,

3) Mean value, which is the average amplitude of the signal across a cycle, reflecting the central tendency of the bioelectrical signal.

4) Standard deviation of the variability or dispersion of the signal amplitude of single-cycle EOG signals, indicating the degree of fluctuation from the mean value.

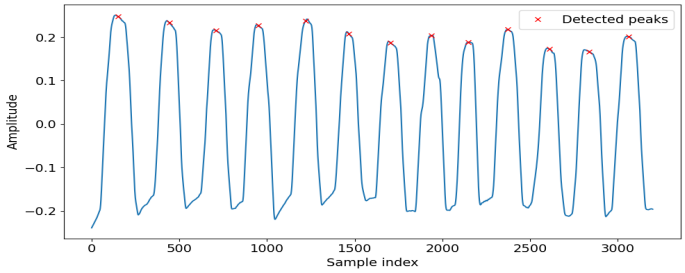

Fig. 3. Single-cycle EOG signal extraction using peak detection.

5) Skewness, which is the asymmetry of the signal distribution in the single-cycle EOG signals, quantifying the extent and direction of deviation from a normal distribution of the bioelectrical signal.

6) Kurtosis, which measures the "tailedness" of the signal distribution in the single-cycle EOG signals, assessing the presence of outliers and the peak sharpness of the bioelectrical signal.

7) Dominant frequency, which is the frequency with the highest power in the single-cycle EOG signal, identifying the predominant oscillatory component present in that time frame.

D. SMOTE algorithm, data segmentation and splitting

The initial dataset exhibited imbalanced and inadequate samples among all the classes, which can result in a biased training of the algorithm. This was resolved using the Synthetic Minority Over-sampling Technique (SMOTE) [17] to create a balanced dataset of 300 samples per class. During data augmentation, it is important to ensure that the upsampled data does not exhibit significant differences. This is because the features are inherently stable for bioelectrical signals due to the consistent nature of physiological processes and homeostatic regulation. If the upsampled data exhibits significant differences, it could lead to the generation of unrealistic or distorted features that may not accurately represent the true characteristics of bioelectrical signals. This inconsistency may result in poor model performance, as the model could learn to recognize artificial patterns that do not exist in real-world data, ultimately compromising its accuracy and generalizability in practical applications. To ensure the integrity of the upsampled data, we calculated the p-value for each class which is shown in Table. I

TABLE I
SAMPLE SIZE FOR THE INDIVIDUAL CLASSES

Classes	Before SMOTE	After SMOTE	P-value
Blink	76	300	0.72
Left	38	300	0.93
Right	62	300	0.95
Up	87	300	0.85
Down	60	300	0.62
UpLeft	80	300	0.90
UpRight	64	300	0.55
DownLeft	70	300	0.80
DownRight	94	300	0.99

As shown in Table I, the p-values are greater than 0.05, indicating no significant differences between the augmented and original dataset, thereby confirming the reliability of the upsampled dataset. The dataset was then divided into three distinct segments: Composite-gaze, Left-gaze, and Right-gaze to ensure robust and accurate training. The specific classes within each segment are detailed in Table.II. The data for each segment was then split into 90% for training and 10% for validation purposes.

TABLE II
DATA SEGMENTATION ACCORDING TO THE CASCADED ARCHITECTURES.

Segment	Classes	Samples
Composite-gaze	Blink	300
	Up	300
	Down	300
	Combined Left & Right gaze	1800
Right-gaze	Right	300
	DownRight	300
	UpRight	300
	Left-gaze	900
Left-gaze	Left	300
	DownLeft	300
	UpLeft	300

E. Feature Scaling

Feature scaling is crucial for normalizing independent variables in a dataset, ensuring that features with larger magnitudes don't overshadow those with smaller ones [18]. This balance enhances model accuracy and efficiency, as well as ensures that features like mean, standard deviation, and range are consistently scaled across both training and test data, thereby maintaining predictive accuracy.

F. Artificial Neural Network (ANN) and Convolutional Neural Network (CNN)

ANN is a machine-learning algorithm inspired by the human brain's neural structure [19]. It comprises interconnected neurons distributed among the input, hidden, and output layers. The input layer processes raw data, the hidden layers extract complex patterns, and the output layer generates the prediction.

On the other hand, CNN is a deep learning algorithm inspired by the visual processing system of the human brain, specifically designed for pattern recognition tasks. CNN has a specialized architecture that utilizes weight sharing and extracts features layer by layer that reduces the number of parameters for faster computations, convergence, and decision-making [20]. CNN architecture consists of multiple layers, each serving a unique function: the Input Layer receives data, the Convolutional Layer applies filters to extract features, and the Pooling Layer reduces the dimension of the feature maps. The fully connected layer classifies these features, and the output layer generates the final result. Furthermore, there are some additional layers such as normalization layers that improves the training stability and convergence, and activation layers that incorporated non-linearity into the network (e.g., ReLU, sigmoid, tanh).

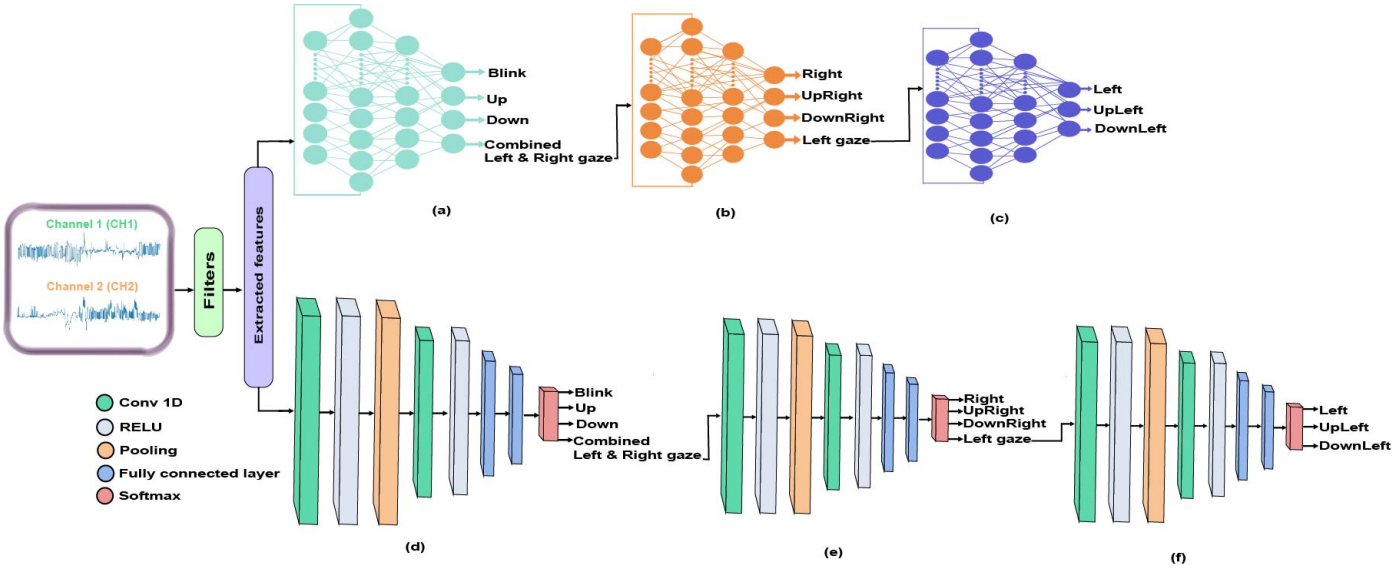

Fig. 4. Cascaded module architectures (a) ANN-1 (b) ANN-2 (c) ANN-3 (d) CNN-1 (e) CNN-2 (f) CNN-3

G. Cascaded architecture

To construct the cascaded modules for both ANN and CNN we used a consistent design across both modules as illustrated in Fig. 4. The first model is used to classify the 4 primary classes from composite gaze, as presented in Table. II. If this model identifies the class as 'Combined Left & Right gaze,' the second model is then activated to further classify among the 4 classes within the right gaze. If the classification pertains to the 'Left-gaze,' the final model is triggered to differentiate among the 3 classes specific to the left gaze.

III. Results and Discussion

The study commenced with the acquisition of EOG signals corresponding to nine distinct ocular movements using six electrodes representing two channels, horizontal (CH1) and vertical (CH2), from a cohort of 20 individuals ensuring equal gender representation, conducted at the KUET biomedical engineering lab with a sampling frequency of 125 Hz.

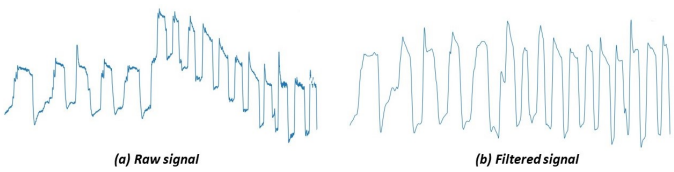

Fig. 5. (a) Example of a recorded EOG signal. (b) EOG signal after applying a low-pass and a high-pass filter to denoise and detrend, respectively.

Analyzing Fig 5 (a), it can be seen that the acquired signals exhibited a significant amount of noise, artifacts, and low-frequency drifts often referred to as trends that must be removed to extract the exact signal associated with the eye movement. At first, a Moving Average low-pass filter with a window size of 30 was used to reduce the high-frequency noise and artifacts. This was followed by a 5th-order Butterworth high-pass filter with a cutoff frequency of 0.2 Hz to remove the trends. The 5th-order design ensures a vertical roll-off while minimizing signal distortion, and the cutoff frequency effectively filters out slow drifts, as illustrated in Fig. 5 (b).

To classify the EOG signals using only single cycles, we created a function that detects the peaks of the signals by comparing them to a threshold of -0.02 V, with a minimum peak distance of 40 samples as explained in section II-C. The parameters mentioned were obtained heuristically. Once the peaks were identified, we extracted 140 data points on either side of the peak to collect that individual cycle data. Using the single cycles data, we constructed a dataset consisting of 14 features, 7 features derived from each channel as outlined in Section II-C. This dataset was then balanced as mentioned in the earlier section.

To gain a deeper insight into the dataset, we computed the correlation matrix that provides correlations between the input and the output parameters with the coefficient ranging from +1 to -1, where +1 indicates a strong positive relationship, -1 indicates a strong negative relationship, and 0 represents no linear correlation. In Fig. 6, we can observe several significant correlations: CH1 max and CH1 mean show a strong positive correlation (0.95), as do CH1 std and CH1 mean (0.98), CH1 std and CH1 max (0.94), CH2 std and CH2 mean (0.97), and CH2 max and CH2 mean (0.74). On the other hand, strong negative correlations were found between CH1 std and CH1 min (-0.90), CH1 min and CH1 mean (-0.88), and CH2 std and CH2 min (-0.89). These correlations demonstrate important patterns within the dataset, providing essential insights for subsequent analysis and predictive modeling.

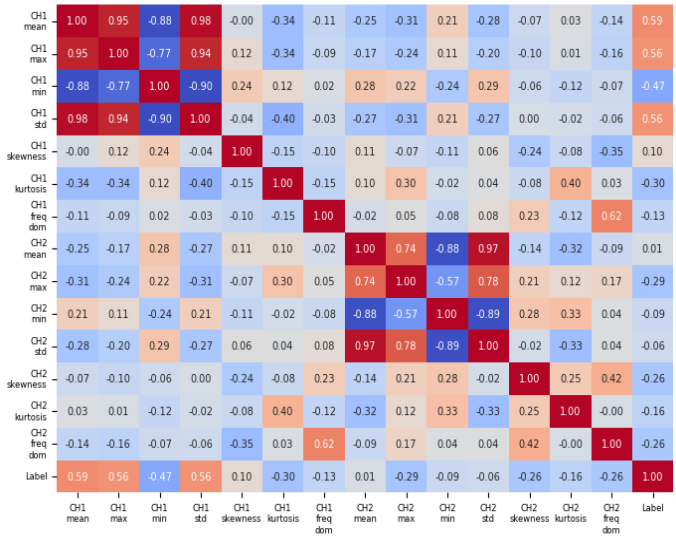

Fig. 6. Correlation matrix: CH1 and CH2 denote channels 1 and 2, with red and blue shades indicating positive and negative correlations respectively.

For rest of the study, this dataset was segmented into three distinct categories: composite gaze, right-gaze, and left-gaze as shown in Table. II. Each segment was then split in a ratio of 90:10 where 90% was used for training neural networks and the remaining 10% was reserved for evaluation purposes. A standard scaler was implemented to normalize the data, avoid any biasing, and ensure all the features contribute equally to the model's performance.

To classify ocular activities based on single-cycle EOG signals while ensuring a minimal amount of latency, we have evaluated two different modules: Cascaded Artificial Neural Networks (ANN) and Cascaded Convolutional Neural Networks (CNN). For each module, we designed particular models relying on the segments, they are ANN-1, ANN-2, ANN-3 similarly CNN-1, CNN-2, and CNN-3. All of the ANN models were designed using a similar architecture consisting of 1 input layer, 2 hidden layers, and 1 output layer with the number of nodes 14, 30, 16, and 4 respectively except for ANN-3, which has an adjustment with the output node set to 3. For our CNN models, we designed a simple architecture. The input layer consists of a 1D convolutional layer (Conv1D) with 35 filters and a kernel size of 3 followed by a max pooling layer (MaxPooling1D) with a pool size of 2. Next, we include a second convolutional layer with 17 filters and a kernel size of 2, and then the output is flattened. This flattened output is passed to a fully connected layer with 8 nodes. The model is concluded with a 4-node output layer utilizing softmax activation, although the CNN-3 has a slight modification, with the output node set to 3. All of the models were compiled using the Adam optimizer, with sparse categorical cross-entropy as the loss function and accuracy as the performance metric. The models were trained with a batch size of 32 for 200 epochs.

During the validation phase, our primary concern was to ensure the models did not exhibit overfitting. To assess overfitting we used the validation loss curve. In cases of overfitting, the validation loss would increase after a certain number of epochs while the training loss continued to decrease indicating that the model was capturing noise and outliers specific to the training data. On the other hand, if the validation loss remained stable or decreased alongside the training loss, it indicates that the models were generalizing well to unseen data and not overfitting.

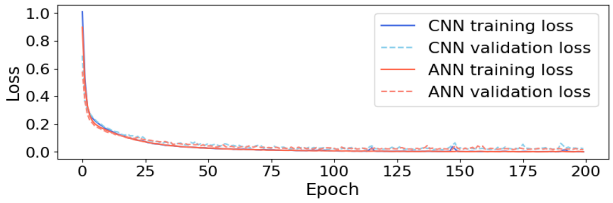

Fig. 7. Epoch-wise variation of training and validation loss.

From Fig. 7, it is evident that the validation loss remains relatively stable across the epochs, indicating that neither the ANN nor the CNN models exhibited overfitting. Then the cascaded modules were subsequently validated using the sample dataset, and their performance is detailed in Table. III.

TABLE III
PERFORMANCE METRICS FOR INDIVIDUAL MODELS AND CASCADED MODULES.

Models	Accuracy	Precision	Recall	F1-Score	Training Time	Validation Time
ANN-1 (Lateral)	99.63%	99.26%	99.86%	99.56%	61.52s	1.19ms
ANN-2 (Right)	97.77%	97.80%	97.77%	97.77%	53.98s	0.89ms
ANN-3 (Left)	100%	100%	100%	100%	47.22s	1.69ms
ANNs Cascaded Module	**99.63%**	**99.64%**	**99.63%**	**99.63%**	**162.72s**	**248.03ms**
CNN-1 (Lateral)	98.88%	98.90%	98.88%	98.88%	63.99s	0.52ms
CNN-2 (Right)	95.55%	95.69%	95.55%	95.55%	52.66s	0.48ms
CNN-3 (Left)	98.88%	98.71%	98.96%	98.82%	35.51s	0.55ms
CNNs Cascaded Module	**99.26%**	**99.29%**	**99.26%**	**99.26%**	**152.16s**	**198.48ms**

Note Validation time quantified on a per-sample basis.

The performance metrics of our cascaded modules show that the ANN module achieved an accuracy, precision, recall, and F1-score of 99.63%, 99.64%, 99.63%, and 99.63%, respectively. The latency of ANN was 248.03 ms per eye movement prediction. CNN module achieved similar metrics with accuracy, precision, recall, and F1-score of 99.26%, 99.29%, 99.26%, and 99.26%, respectively. However, it

demonstrated a superior latency, requiring only 198.48 ms per eye movement prediction.

In comparison to the average human reaction time of 226.66 ms to 276.7 ms [13], CNN demonstrates a superior latency that is well below the average reaction time. This can be attributed to its architectural design rather than differences in processing time. The CNN architecture utilizes convolutional layers for localized feature extraction, similar to memory operations in Linear Time-Invariant (LTI) systems. These operations effectively capture essential features by summing over localized regions of the input, reducing the dimensionality of the data and resulting in fewer parameters to train compared to the fully connected layers in ANN. As a result, the CNN module not only achieved human-level precision but also exceeded human reaction time. This makes it exceptionally suitable for real-time applications where rapid and accurate processing is crucial.

IV. Conclusion

In this study, we experimentally demonstrate the potential of cascaded neural network architectures that can successfully classify a wide range of eye movements based on the statistical features of single-cycle EOG signals and with a prediction time faster than the average reaction time of a human being. Using a methodical & robust signal processing procedure along with cascaded architectures, we achieved a classification accuracy, precision, recall & and F1-score close to 100% for both the ANN and CNN algorithms. Moreover, the cascaded ANN exhibited a latency of 248 ms whereas the cascaded CNN demonstrated a superior lower latency of 198 ms, which is well below the average human reaction time of 250 ms. This can be attributed to the pooling layers after convolutions, and weights sharing across different parts of the input. Our proposed method will provide timely feedback & take corrective actions suitable for real-time applications, especially in critical assistive technologies such as in the control of wheelchairs, automobiles, and robotic-assisted surgery, where immediate and precise control is necessary. This will ensure a seamless HCI system that will significantly lower the risk of accidents caused by delayed responses.

References

[1] M. I. Rusydi, A. U. Baiqi, M. A. Rahman, A. Jordan, H. Nugroho, K. Matsushita, S. Syafii, Y. A. R. Sari, N. Windasari, A. W. Setiawan, et al., "Electrooculography signal as alternative method to operate wheelchair based on SVM classifier," in Proc. AIP Conf., vol. 2891, no. 1, 2024.

[2] R. J. Doniec, N. Piaseczna, K. Duraj, S. Sieciński, M. T. Irshad, I. Karpiel, M. Urzeniczok, X. Huang, A. Piet, M. A. Nisar, et al., "The detection of alcohol intoxication using electrooculography signals from smart glasses and machine learning techniques," in Proc. Systems and Soft Computing, vol. 6, p. 200078, 2024, Elsevier.

[3] Q. Huang, Y. Chen, Z. Zhang, S. He, R. Zhang, J. Liu, Y. Zhang, M. Shao, and Y. Li, "An EOG-based wheelchair robotic arm system for assisting patients with severe spinal cord injuries," in Proc. Journal of Neural Engineering, vol. 16, no. 2, p. 026021, 2019, IOP Publishing.

[4] A.-u. Kabir, F. B. Shahin, and M. K. Islam, "Design and implementation of an EOG-based mouse cursor control for application in human-computer interaction," in Proc. Journal of Physics: Conf. Series, vol. 1487, no. 1, p. 012043, 2020, IOP Publishing.

[5] I. N. SM, X. Zhu, Y. Chen, and W. Chen, "Sleep stage classification based on EEG, EOG, and CNN-GRU deep learning model," in Proc. 2019 IEEE 10th Int. Conf. Awareness Science and Technology (iCAST), 2019, pp. 1–7.

[6] S. N. Hernández Pérez, F. D. Pérez Reynoso, C. A. González Gutiérrez, M. D. L. Á. Cosío León, and R. Ortega Palacios, "EOG signal classification with wavelet and supervised learning algorithms KNN, SVM, and DT," in Proc. Sensors, vol. 23, no. 9, p. 4553, 2023.

[7] C.-T. Lin, J.-T. King, P. Bharadwaj, C.-H. Chen, A. Gupta, W. Ding, and M. Prasad, "EOG-based eye movement classification and application on HCI baseball game," IEEE Access, vol. 7, pp. 96166–96176, 2019.

[8] R. Ileri, F. Latifoğlu, and E. Demirci, "A novel approach for detection of dyslexia using convolutional neural network with EOG signals," Med. Biol. Eng. Comput., vol. 60, no. 11, pp. 3041–3055, 2022.

[9] M. R. Pratomo, B. G. Irianto, T. Triwiyanto, B. Utomo, E. D. Setioningsih, and D. Titisari, "Prosthetic hand with 2-dimensional motion based EOG signal control," in Proc. IOP Conf. Ser. Mater. Sci. Eng., vol. 850, no. 1, p. 012024, 2020.

[10] A.-u. Kabir, F. B. Shahin, and M. K. Islam, "Design and implementation of an EOG-based mouse cursor control for application in human-computer interaction," in Proc. J. Phys. Conf. Ser., vol. 1487, no. 1, p. 012043, 2020.

[11] K. S. Roy and S. M. R. Islam, "An RNN-based hybrid model for classification of electrooculogram signal for HCI," IJC, vol. 22, no. 3, pp. 335–344, 2023.

[12] R. Hossieny, M. Tantawi, M. F. Tolba, and others, "Developing a method for classifying electro-oculography (EOG) signals using deep learning," Int. J. Intell. Comput. Inf. Sci., vol. 22, no. 3, pp. 1–13, 2022.

[13] A. Jain, R. Bansal, A. Kumar, and K. D. Singh, "A comparative study of visual and auditory reaction times on the basis of gender and physical activity levels of medical first year students," Int. J. Appl. Basic Med. Res., vol. 5, no. 2, pp. 124–127, 2015, Medknow.

[14] K. Glavas, K. D. Tzimourta, A. T. Tzallas, N. Giannakeas, and M. G. Tsipouras, "Empowering individuals with disabilities: A 4-DoF BCI wheelchair using MI and EOG signals," IEEE Access, 2024.

[15] J. K. Zao, T.-P. Jung, H.-M. Chang, T.-T. Gan, Y.-T. Wang, Y.-P. Lin, W.-H. Liu, G.-Y. Zheng, C.-K. Lin, C.-H. Lin, et al., "Augmenting VR/AR applications with EEG/EOG monitoring and oculo-vestibular recoupling," in Proc. 10th Int. Conf. Foundations of Augmented Cognition: Neuroergonomics and Operational Neuroscience, HCI International 2016, Toronto, ON, Canada, Jul. 17-22, 2016, pp. 121–131, Springer, 2016.

[16] Y. Tian and J. Cao, "Fatigue driving detection based on electrooculography: A review," EURASIP J. Image and Video Process., vol. 2021, no. 1, p. 33, 2021.

[17] N. V. Chawla, K. W. Bowyer, L. O. Hall, and W. P. Kegelmeyer, "SMOTE: Synthetic minority over-sampling technique," J. Artif. Intell. Res., vol. 16, pp. 321–357, 2002.

[18] M. M. S. Raihan, A. B. Shams, and R. Bin Preo, "Multi-class electrogastrogram (EGG) signal classification using machine learning algorithms," in Proc. 2020 23rd Int. Conf. Comput. and Inf. Technol. (ICCIT), Dhaka, Bangladesh, 2020, pp. 1–6.

[19] J. Zupan, "Introduction to artificial neural network (ANN) methods: What they are and how to use them," Acta Chim. Slovenica, vol. 41, no. 3, p. 327, 1994.

[20] L. Alzubaidi, J. Zhang, A. J. Humaidi, A. Al-Dujaili, Y. Duan, O. Al-Shamma, J. Santamaría, M. A. Fadhel, M. Al-Amidie, and L. Farhan, "Review of deep learning: Concepts, CNN architectures, challenges, applications, future directions," J. Big Data, vol. 8, p. 1–74, 2021, Springer.